



HAL
open science

Damping model-free analysis of a stochastic multi-scale frame element for earthquake engineering applications

Pierre Jehel, Hugues Vincent, Thomas Rodet

► To cite this version:

Pierre Jehel, Hugues Vincent, Thomas Rodet. Damping model-free analysis of a stochastic multi-scale frame element for earthquake engineering applications. International Conference on Computational Stochastic Mechanics (CSM-7), G. Deodatis and P. D. Spanos, Jun 2014, Santorini, Greece. 10.3850/978-981-09-5348-5_033 . hal-01071341

HAL Id: hal-01071341

<https://centralesupelec.hal.science/hal-01071341>

Submitted on 2 Aug 2018

HAL is a multi-disciplinary open access archive for the deposit and dissemination of scientific research documents, whether they are published or not. The documents may come from teaching and research institutions in France or abroad, or from public or private research centers.

L'archive ouverte pluridisciplinaire **HAL**, est destinée au dépôt et à la diffusion de documents scientifiques de niveau recherche, publiés ou non, émanant des établissements d'enseignement et de recherche français ou étrangers, des laboratoires publics ou privés.

DAMPING MODEL-FREE ANALYSIS OF A STOCHASTIC MULTI-SCALE REINFORCED CONCRETE FRAME ELEMENT FOR EARTHQUAKE ENGINEERING APPLICATIONS

PIERRE JEHEL^{1,3}, HUGUES VINCENT^{2,3} and THOMAS RODET²

¹*Laboratoire MSSMat (UMR CNRS 8579), École Centrale Paris, Grande voie des Vignes, 92290 Châtenay-Malabry, France.*

E-mail: pierre.jehel@ecp.fr

²*Laboratoire SATIE (UMR CNRS 8029), ENS Cachan, 61 avenue du Président Wilson, 94230 Cachan, France.*

³*Department of Civil Engineering and Engineering Mechanics, Columbia University, 630 SW Mudd, 500 West 120th Street, New York, NY, 10027, USA.*

The viscous damping forces commonly added in earthquake engineering applications lack a sound physical justification. Consequently, whether or not they accurately represent what they are added for is uncertain. In this paper, this latter source of uncertainty is removed, appealing to the concept of discrepancy forces, in the analysis of the capabilities of a nonlinear reinforced concrete frame elements to represent actual seismic behavior. Frame elements are modeled as fiber elements accommodating uniaxial concrete and steel behavior laws; two different nonlinear cyclic concrete behavior laws are considered: a stochastic multi-scale concrete model along with a more classical one. Concrete parameters are identified from experimental data using Bayesian inference technique. Finally, the capabilities of the two models to represent the actual response of a reinforced concrete frame element tested on a shaking table are compared in an objective way, that is without any side effect resulting from the action of uncertain damping forces.

Keywords: Earthquake engineering, damping, stochastic multi-scale material model, frame structure, discrepancy forces, Bayesian inference.

1 Introduction

For running accurate predictive computational analyses of nonlinear structures in seismic loading, practitioners have to cope with the dual issue of i) explicitly modeling the main seismic energy absorption mechanisms in the structural model, and ii) adding damping forces that represent all the energy dissipative mechanisms that are not otherwise accounted for in the inelastic structural model. There is no structural model which is always capable of perfectly grasping altogether the numerous energy dissipative mechanisms activated in inelastic structures in seismic motion. Consequently, the addition of damping forces necessarily lacks a sound physical justification and whether or not those forces accurately represent what they are added is uncertain.

More specifically, denoting \mathbf{u} the displacement field and using an upper dot to represent time derivation, basic equilibrium equation for solving earthquake engineering problems read:

$$\mathbf{f}^{ine}(\ddot{\mathbf{u}}; t) + \mathbf{f}^{dam}(\dot{\mathbf{u}}; t) + \mathbf{f}^{hys}(\mathbf{u}; t) = \mathbf{f}^{ext}(t) \quad (1)$$

In addition to the inertia (\mathbf{f}^{ine}), resisting (\mathbf{f}^{hys}) and seismic along with static external (\mathbf{f}^{ext}) forces, it is common practice to add viscous damping forces (\mathbf{f}^{dam}) “to simulate the portion of energy dissipation arising from both structural and nonstructural components (e.g., cladding, partitions) that is not otherwise incorporated in the model” (FEMA P695, 2009, §6.4.4.). In inelastic time history analyses, such damping models are not built on a sound physical basis but rather following an ad hoc method

Damping model-free analysis of a stochastic multi-scale frame element for earthquake engineering
 P. Jehel, H. Vincent, and T. Rodet

allowing for adding dissipation in the system while remaining easy to be implemented (see the studies on Rayleigh damping in Jehel et al. (2014); Charney (2008); Hall (2006)).

In the case of reinforced concrete structures, there is abundant literature on concrete models that have been developed and implemented in structural elements in the purpose of grasping the salient features of concrete response in seismic loading as a step toward, ultimately, computing accurate forces $\mathbf{f}^{hys}(t)$. This is the topic of section 2 in this paper where two types of uniaxial concrete models to be implemented in fiber elements will be briefly introduced: a stochastic multi-scale model along with a more classical phenomenological model with internal variables.

When running numerical inelastic time history analyses and then comparing model outputs with experimental measures to assess the validity of a simulation, one actually checks the validity of the combined action of both the structural (\mathbf{f}^{hys}) and the damping (\mathbf{f}^{dam}) forces altogether. Determining which of the inelastic structural model or the damping model is accurate, or which is not, is a kind of chicken-and-egg problem. Indeed $\mathbf{f}^{hys}(\mathbf{u})$ and $\mathbf{f}^{dam}(\dot{\mathbf{u}})$ are interdependent due to the fact that the displacement field is affected by both the structural and the damping model, making it practically impossible to determine whether a poor overall model response is due to a poor structural model or to a poor damping model. As a consequence, in case the accuracy of $\mathbf{f}^{hys}(\mathbf{u})$ only has to be investigated, it is important to carry out a damping model-free analysis. This is desirable for instance to compare the respective capabilities of two different concrete behavior laws to represent actual seismic nonlinear response of a frame element. To that purpose, the concept of discrepancy forces will be introduced in the third section of this paper.

Before closing the paper with some conclusions, numerical applications will be presented. The parameters of the two concrete behavior laws introduced in section 2 will be identified with Bayesian inference technique and then, the discrepancy forces pertaining to one column of a reinforced concrete frame tested on

a shaking table will be computed. This provides a damping model-free comparison of the respective performances of both concrete models in structural inelastic time history seismic analysis, that is a comparison that is not possibly biased by the effects of uncertain damping forces.

2 Uniaxial concrete behavior laws

2.1 Uniaxial concrete response in compressive cyclic loading

In the earthquake engineering community, there is an abundant literature on the formulation and numerical implementation of material models developed for representing the main features of concrete response in cyclic loading. Typical axial stress with respect to axial strain response of a concrete specimen in cyclic compressive loading is depicted in figure 1. We provide here a few references to illustrate four particular categories of concrete models:

- (i) Analytical stress-strain relations (power laws, exponential laws,...) identified from experimental observations (e.g. Wong and Vecchio (2002); Computers & Structures Inc. (2007)).
- (ii) Stress-strain phenomenological laws derived from thermodynamical principles with internal variables (see e.g. Richard and Ragueneau (2013); Jehel et al. (2010)). This can be interpreted as a multi-scale approach, as by Maugin (1999), in the sense that the internal variables, which are the history of the concrete response, convey at macro-scale the effects of mechanisms occurring at lower scales.
- (iii) Probabilistic elasto-plasticity model based on the computation of the time evolution of the probability density function of the stress (e.g. Jeremić et al. (2007)).
- (iv) Concrete meso-scale (aggregates, cement paste and so-called interfacial transition zone around aggregate grains) is explicitly represented as a spatial truss with enhanced kinematics within the finite element method, for instance in the work

of Benkemoun et al. (2010). Due to the computation costs, the approach is not tractable for structural analyses but it is interesting to observe that characteristic features of the uniaxial concrete response at macro-scale can be explained by this representation of concrete meso-scale.

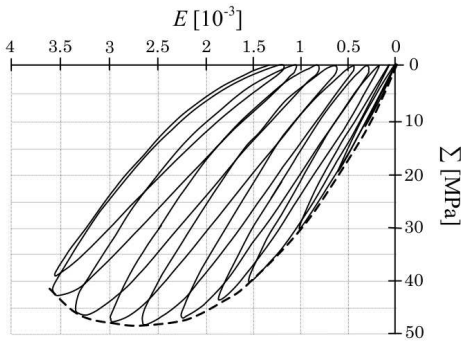


Figure 1: Strain-stress concrete experimental response in pseudo-static cyclic compressive loading (adapted from a figure by Ramtani (1990)). Σ is the (homogeneous) compression stress in a concrete test specimen, that is the load in the hydraulic cylinder of the testing machine divided by the area of the specimen cross section; E is the homogeneous deformation field, that is the displacement of the cylinder divided by the specimen height.

At structural level, those concrete laws can be integrated in 2D/3D finite elements. For earthquake engineering applications, the fiber element approach, as described e.g. by Davenne et al. (2003), is particularly well adapted because it provides a good compromise between computational efficiency and refined description of the physics. Implemented with displacement-based formulation and Euler-Bernoulli kinematics assumption, fiber elements call for 1D material behavior law at each numerical integration point in the control sections of the beam (for another beam element formulation, see e.g. the work of Taylor et al. (2003)).

Virtual internal potential increment for such a beam element of length L and section S is

numerically approximated as:

$$\begin{aligned} \delta W^{int} &:= \int_L \int_S \delta E(\mathbf{x}) \Sigma(\mathbf{x}) dS dx_1 \\ &\approx \sum_{l=1}^2 \sum_{F=1}^{N^F} A^F \delta E_l^F \Sigma_l^F W_l \end{aligned} \quad (2)$$

where A^F is the cross section area, E_l^F and Σ_l^F are the axial strain and stress in fiber F in control section l , and W_l denotes quadrature weight and length. $\Sigma^F = \hat{\Sigma}(E^F)$ is the uniaxial behavior law of fiber F material, which, in reinforced concrete structures, is either concrete or steel. In common practice, concrete is considered as homogeneous over the beam so that $\hat{\Sigma}(\mathbf{x})$ is the same concrete law at any material point \mathbf{x} in the beam. The number of fibers N^F has to be sufficiently large for the structural response of the model to be independent of it.

2.2 A uniaxial stochastic multi-scale nonlinear cyclic concrete law

Thereafter, we will consider another type of concrete material model, which we refer to as “multi-scale stochastic” because it is based on the homogenization of a randomly generated heterogeneous structure at a meso-scale. A detailed description of the model can be found in Jehel and Cottreau (2015). The principal motivation for developing such an approach comes from the fact that concrete exhibits a “continuous range of micro-structural dimensions”, as stated by Stroeven et al. (2008), when observed with progressive magnification. At first glance, with human eyes, the bi-phasic nature of concrete is obvious (mixture of aggregates and cement paste). Then, zooming in the cement paste would reveal other heterogeneities so that several other phases would appear at microscopic scale (water, pores, air voids, C-S-H, CH, ettringite,...).

Seeking meaningful information in these heterogeneities to explain characteristic features of the concrete response at macro-scale looks compelling. However, there is obviously both too little knowledge, from a physical point of view, and too much data to process, from a computational viewpoint, to realistically think

Damping model-free analysis of a stochastic multi-scale frame element for earthquake engineering
P. Jehel, H. Vincent, and T. Rodet

about a computer program that would explicitly account for the full range of concrete micro-structures in structural engineering applications. As a trade-off, we propose an approach based on the following set of assumptions (we refer the reader to Jehel and Cottreau (2015) for further details):

- (i) Concrete uniaxial homogeneous response at macro-scale $\Sigma = \hat{\Sigma}(E)$ results from uniaxial heterogeneous behavior at meso-scale $\sigma = \hat{\sigma}(\epsilon(\mathbf{x}))$, such that:

$$\begin{aligned} \Sigma_l^F &:= \hat{\Sigma}(E_l^F) = \frac{1}{|\mathcal{R}|} \int_{\mathcal{R}} \hat{\sigma}(\epsilon_l^F) d\mathcal{R} \\ &\approx \frac{1}{N_f^2} \sum_{f=1}^{N_f^2} \hat{\sigma}(\epsilon(\mathbf{x}_l^{F,f})) \end{aligned} \quad (3)$$

where $|\mathcal{R}|$ is the size of a representative square area \mathcal{R} divided into $N_f \times N_f$ equal square parts, and

$$\epsilon(\mathbf{x}_l^{F,f}) = E(\mathbf{x}_l^F) \quad \forall \mathbf{x}_l^{F,f} \in \mathcal{R} \quad (4)$$

- (ii) Concrete meso-scale response is represented by an elasto-plastic law with linear kinematic hardening. At any material point, yielding is parameterized by the yield stress σ_y . This is achieved using classical computational model with internal variables (Simo and Hughes (1998)).
- (iii) The heterogeneity at meso-scale is conveyed by the fluctuations of the yield stress $\sigma_y(\mathbf{x})$, as depicted in figure 2. These fluctuations are represented by a 2D homogeneous log-normal stochastic field over \mathcal{R} , built as the translation of a Gaussian field generated with the Spectral Representation Method as presented by Shinozuka and Deodatis (1996), and with triangular power spectral density function.
- (iv) Concrete has no strength in tension.

Figure 3 shows macroscopic response at each numerical integration point \mathbf{x}_l^F in the beam. This has been computed with $N_f = 64$, $|\mathcal{R}| = d \times d$, correlation length in both orthogonal directions $\ell_c = d/10$. We refer the reader

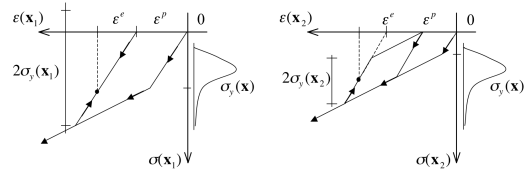


Figure 2: Compressive cyclic behavior at meso-scale. The yield stress $\sigma_y(\mathbf{x})$ fluctuates over the concrete representative section \mathcal{R} : two local responses at two distinct material points \mathbf{x}_1 [left] and \mathbf{x}_2 [right] are represented in the figure.

to Jehel and Cottreau (2015) for further discussion on the choice of these parameters. This set of parameters will remain unchanged for any result shown throughout this paper. It is obvious in figure 3 that the homogenized response at macro-scale exhibits much richer behavior than the local response at meso-scale (see figure 2). An interesting feature is in particular the hysteresis during unloading-reloading cycles. Besides, figure 3 shows that \mathcal{R} is a representative area in the sense that there is practically independence between the random realization of the meso-structure and the response at macro-scale.

As already appealed for by Charmpis et al. (2007), albeit in a different context, there is a need here for interaction between structural and material scientists so that the assumptions made to account for the heterogeneous nature of concrete at meso-scale be supported by experimental observations.

2.3 A uniaxial concrete law with internal variables

A second kind of concrete model will also be used in the numerical application that follows. This model is based on the work presented in Jehel et al. (2010) where a uniaxial material model is developed in the framework of thermodynamics with internal variables, along with enhanced kinematics accommodating discontinuities in the displacement field. The model is capable of representing salient phenomena that can be experimentally observed in the stress-strain response of a concrete representative elementary volume in cyclic uni-

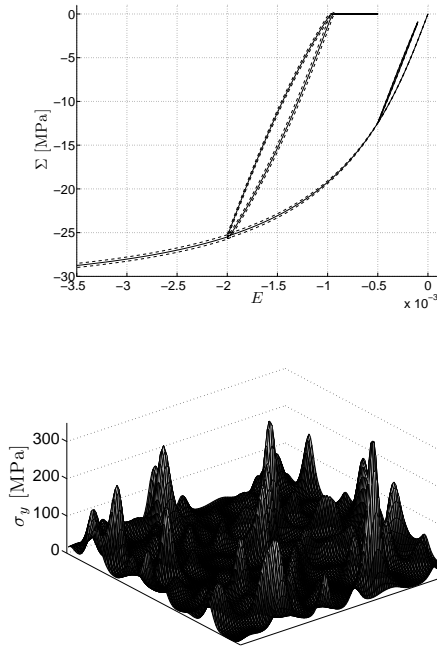


Figure 3: [top] Mean (—) along with mean plus and minus standard deviation (- -) response at macro-scale obtained from a sample of 2,000 meso-structures. [bottom] One realization of concrete meso-structure. Targeted mean and standard deviation of the marginal log-normal law are $\mu = 35.0$ MPa and $s = 51.9$ MPa. This figure shows in particular that, for the parameterization of the meso-scale chosen, concrete response at macro-scale almost is independent of the realization of the meso-structure.

axial loading (see figure 4): brittle behavior in tension, quasi-brittle behavior in compression with strain hardening, appearance of residual deformation, stiffness and strength degradations, hysteresis in unloading-reloading cycles. Besides, the model is designed for accommodating loading-rate dependent effects. To control these mechanisms altogether, 10 internal variables and a set of 13 parameters are required. Not all the capabilities of the model will be exploited thereafter in order to reduce the number of parameters to handle.

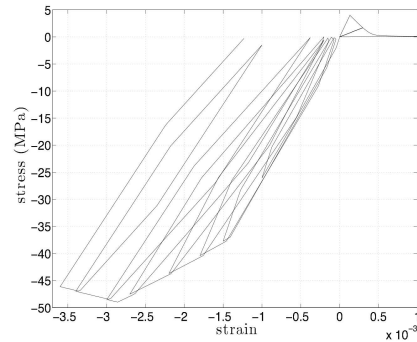


Figure 4: Stress (Σ)-strain (E) concrete response at macro-scale obtained using the model developed in Jehel et al. (2010) in the framework of thermodynamics with internal variables.

3 Damping model-free analysis of structural seismic response

Now, we want to compare this two concrete models regarding their capability of grasping the physical inelastic mechanisms occurring in structural time history inelastic seismic simulations. The question which is at stake here is about defining a strategy to have an objective comparison of both concrete material models. As will be illustrated in this section, in earthquake engineering problems where experimental data only is available from seismic tests, the answer to this issue is not that obvious because of the common addition of Rayleigh damping forces in the numerical model “to simulate the portion of energy dissipation arising from both structural and nonstructural components (e.g., cladding, partitions) that is not otherwise incorporated in the model” (FEMA P695, 2009, §6.4.4.). This latter “model” being here the inelastic structural elements that incorporate either of the concrete models presented in previous section.

3.1 Classical formulation of a nonlinear structural earthquake engineering problem

The classical formulation for time-history analysis of nonlinear structure in seismic motion reads, in its digitized form: At each time step t_n , find the relative displacement, velocity

Damping model-free analysis of a stochastic multi-scale frame element for earthquake engineering
 P. Jehel, H. Vincent, and T. Rodet

and acceleration fields $(\mathbf{u}, \dot{\mathbf{u}}, \ddot{\mathbf{u}})$ such that

$$\mathbf{r}(\mathbf{u}, \dot{\mathbf{u}}, \ddot{\mathbf{u}}; t_n) = \mathbf{0} \quad (5)$$

with

$$\mathbf{r} := \mathbf{f}^{ext}(t_n) - (\mathbf{M}\ddot{\mathbf{u}}(t_n) + \mathbf{C}(t_n)\dot{\mathbf{u}}(t_n) + \mathbf{f}^{hys}(\mathbf{u}; t_n)) \quad (6)$$

where \mathbf{M} and \mathbf{C} are the mass and damping matrices while \mathbf{f}^{hys} and \mathbf{f}^{ext} are the inelastic structural response forces and the external (static and seismic) loading vectors.

The assumption of Rayleigh damping is generally made to calculate the viscous forces:

$$\mathbf{C}(t_n) = \alpha \mathbf{M} + \beta \mathbf{K}(t_n) \quad (7)$$

where $\mathbf{K} = \partial \mathbf{f}^{hys} / \partial \mathbf{u}$ is the structural tangent stiffness matrix. Coefficients α and β most commonly are set once for all at the beginning of the simulation. Most commonly too, they are identified so that the same modal damping ratio ξ is generated at structural vibration modes I and J , with $I = 1$ and J defined so that 90% or 95% of the structural mass is activated by the first J modes. It has been acknowledged many times that the actual amount of seismic energy dissipated by Rayleigh damping throughout inelastic time-history analyses is difficult to control (see e.g. Jehel et al. (2014); Charney (2008); Hall (2006)). Practically, this means that at a time t_n during the analysis, there is some uncertainty in the value of the actual damping ratio: it can be twice or three times higher or lower than the targeted damping ratio initially set by the user.

The issue here is not to discuss the pros and cons of using Rayleigh damping, but to avoid the bias such a damping model can introduce when comparing two concrete models. Indeed, two different concrete models implemented in the same structural model yield two different resisting forces vectors and, consequently, two different tangent stiffnesses. Then, using two different concrete models — as well as two different meso-structures in the case of the multiscale stochastic concrete model — not only yields two different structural forces vectors (\mathbf{f}^{hys}) but also two different damping forces

vectors $\mathbf{f}^{dam} = \mathbf{C}\dot{\mathbf{u}}$ or, in other words, two different actual modal damping ratios ξ . Comparing the outputs of both simulations thus means comparing two different pairs of inelastic structural model *plus* damping model, not only two different structural models. Hence a comparison of the concrete laws that turns out to be biased by the uncertainty on the actual modal damping ratio.

3.2 Sensitivity of analysis outputs to viscous damping ratio

Then, a natural question is whether or not the outputs of interest in a structural seismic analysis are sensitive to the modal damping ratio generated by Rayleigh damping model.

Lee and Mosalam (2005) run inelastic time history analyses of a reinforced concrete structure with beams, columns and walls modeled by fiber elements. A bilinear stress-strain (1D) relationship is used for the reinforcement steel and a modified Kent-Park stress-strain (1D) relationship with zero tensile strength for concrete fibers. Uncertainties are introduced in the seismic ground motion, in the strength and stiffness of concrete and steel, as well as in the modal damping ratio used to identify the Rayleigh damping coefficients α and β (ξ has truncated Gaussian distribution with a mean of 5% and a COV of 40%). The study reports that for some engineering demand parameters of interest for performance-based design, viscous damping ratio is the second source of uncertainty right after ground motion.

A two-story two-bay reinforced concrete frame structure is modeled in Jehel (2013) with fiber elements accommodating bilinear stress-strain (1D) relationship for the steel rebars and the model introduced above in section 2.3 for concrete fibers. Viscous damping is added in the inelastic time history analyses with Rayleigh model and a random damping ratio uniformly distributed between 1% and 10%. The analysis shows in particular that, for some of the ground motions used, the maximum inter-story drift ratio can be significantly sensitive to the Rayleigh damping ratio.

Ideally, one wants to be able to compare the capabilities of two different concrete material

models to grasp experimentally observed structural behaviors in a way that is independent of any side effect coming from uncertain viscous damping ratio. However, in practice, for earthquake engineering applications, one has generally only access to experimental data from shaking table tests, that is data that one attempts to predict numerically with the addition of uncertain damping forces. The concept of discrepancy forces is introduced right below as a way to circumvent this issue.

3.3 The discrepancy forces as an objective approach for structural model comparison in seismic loading

The concept of discrepancy forces in computational dynamics has been introduced in Jehel (2014) and is briefly presented here. Suppose one has a N -degree-of-freedom (DOF) FE model of a structure that is tested on a shaking table. Then, suppose both the relative displacement and relative acceleration time histories are recorded during the experimental test at $N^e \leq N$ DOFs of the FE mesh of the structure and gathered in vectors $\mathbf{y}^e(t)$ and $\ddot{\mathbf{y}}^e(t)$ of size N^e each. Then, the discrepancy forces are defined as the forces needed in the system to satisfy the dynamic balance equation without the uncertain damping forces vector. Sorting the DOFs so that the N^e free DOFs that are monitored during the experimental test as well as the N^b DOFs that are controlled by imposed boundary conditions are gathered, it comes (see equation (6)):

$$\begin{pmatrix} \mathbf{f}^{dis,e}(t) \\ \mathbf{f}^{dis,f}(t) \\ \mathbf{f}^{dis,b}(t) \end{pmatrix} := \begin{pmatrix} \mathbf{f}^{ext,e}(t) \\ \mathbf{f}^{ext,f}(t) \\ \mathbf{f}^{ext,b}(t) \end{pmatrix} - \mathbf{M} \begin{pmatrix} \ddot{\mathbf{y}}^e(t) \\ \ddot{\mathbf{y}}^f(t) \\ \ddot{\mathbf{y}}^b(t) \end{pmatrix} - \begin{pmatrix} \mathbf{f}^{hys,e}(\mathbf{y}^e, \mathbf{y}^f, \mathbf{y}^b; t) \\ \mathbf{f}^{hys,f}(\mathbf{y}^e, \mathbf{y}^f, \mathbf{y}^b; t) \\ \mathbf{f}^{hys,b}(\mathbf{y}^e, \mathbf{y}^f, \mathbf{y}^b; t) \end{pmatrix} \quad (8)$$

In an ideal situation, the displacement and acceleration time histories would have been recorded for all the DOFs of the FE mesh. Then, $\mathbf{f}^{hys}(\mathbf{y}^e; t)$ could be computed in a quasi-static nonlinear structural analysis, and then, because \mathbf{M} and \mathbf{f}^{ext} are known a priori, the discrepancy forces could all be calculated according to equation (8). However, in

practice, there is usually not such an amount of data recorded and, to compute \mathbf{f}^{dis} , some other assumptions have to be made to cope with this lack of knowledge on the experimental response of the structure. A practical case where the dynamic effects for the N^f DOFs not monitored during shaking table test are neglected is presented in Jehel (2014) as well as, in a simpler case though, in the next section.

Once the discrepancy forces are computed, they provide information on the capability of the structural model to represent the experimental response of the structure or, in other words, the forces that should be added in the system to account for the mechanisms either not or poorly represented by the inelastic structural response \mathbf{f}^{hys} . Discrepancy forces are independent of the damping model and consequently do not carry the uncertainty this latter brings in the analysis.

4 Numerical application

4.1 Shaking table test of a frame structure

Experimental data recorded during the shaking table test of a half-scale ductile moment-resisting reinforced concrete frame is used (see figure 5). Four concrete blocks were used to simulate concentrated gravity loads in every beam span. The N04W component of the ground motion recorded in Olympia, Washington on April 13, 1949 was selected for the test program. Tests have been carried out for two analogous structures designed with two different assumptions: either a shear force reduction factor $R = 2$ or $R = 4$. This latter case is considered in this paper. The detailed presentation of the test and design assumptions can be found in Filiatrault et al. (1998).

Recorded data during shaking table test are the horizontal displacement and acceleration time histories at both floors of the frame, along with the acceleration of the shaking table (seismic ground motion).

4.2 Numerical modeling assumptions

4.2.1 Finite element structural model

Fiber element is used to model one column of the 2D frame structure (see mesh in figure 6).

Damping model-free analysis of a stochastic multi-scale frame element for earthquake engineering
 P. Jehel, H. Vincent, and T. Rodet

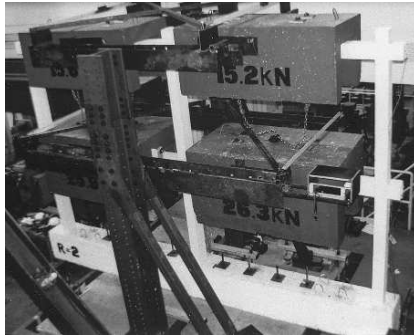


Figure 5: RC frame structure tested on the shaking table at École Polytechnique Montreal. The frame is 5-meter wide (2×2.5 m) and 3-meter high (2×1.5 m). Each beam supports additional masses to account for service static loads.

Column is modeled by two identical elements. Element sections are divided into 8 layers (8×1 fibers). Column is fixed at its base; at its top, 1st-floor horizontal displacement time history recorded during shaking table test is applied while vertical DOF is left free and rotation is assumed to be null. This latter assumption is expected to introduce some error in the results because, during shaking table test, the structural joint rotated. Rotation has not been measured though, hence this hypothesis.

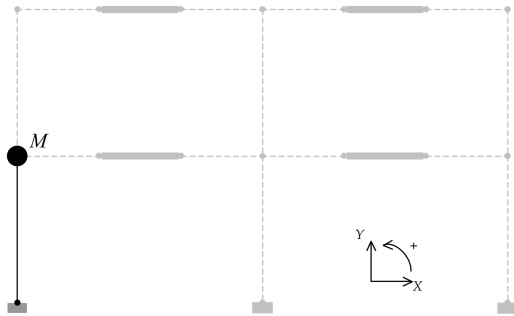


Figure 6: In black: analyzed column of the frame. M concentrates a quarter of the total mass of the frame structure.

4.2.2 Reinforcement steel behavior model

Young modulus $C_s = 224.6$ GPa, yield stress $\Sigma_y = 438$ MPa and ultimate stress $\Sigma_u = 601$ MPa have been experimentally measured

during uniaxial tests on longitudinal steel rebars. An elasto-plastic model with kinematic hardening is used to represent steel response in cyclic loading. The model implemented according to these latter parameters is shown in figure 7.

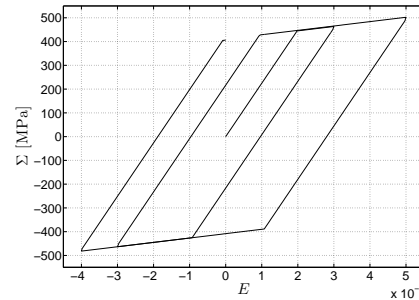


Figure 7: Steel longitudinal rebar constitutive law.

4.2.3 Identification of the concrete models

Uniaxial compression tests have been carried out on specimens of the concrete used to build the frame. According to these data, we use here Young modulus $C_c = 27.5$ GPa and ultimate compression stress $\Sigma'_c = 27.75$ MPa. In the absence of information on the response of confined concrete, we model all the concrete fibers as unconfined, although enhanced ductility properties generally are associated to the fibers inside the stirrups. Besides, in the absence of experimental data in cyclic loading, the identification is performed so that only the backbone curve of the numerical response fits the experimental data.

- (i) For the multi-scale concrete model, referred to as \mathcal{M}_1 in the following, kinematic hardening coefficient H^p at meso-scale is uniform and taken as null. Indeed, this parameter controls the tangent modulus as deformation E becomes large and, concrete tangent modulus can take zero value before softening (softening phase is not modeled here). Then, the remaining parameters to be identified are the mean μ

and standard deviation s of the marginal log-normal law used to generate the random meso-structures. The effects of those two parameters on the response at macro-scale are illustrated in figure 8.

- (ii) Concerning the concrete model presented in section 2.3 above, hereafter referred to as \mathcal{M}_2 , a simplified version of it is used here so that only two parameters have to be identified too. As illustrated in figure 9 [bottom], concrete compressive response is assumed to be first elastic (slope C_c); then, as the stress reaches Σ_f , continuum damage is activated and its evolution is controlled by parameter K^d ; finally, once Σ'_c has been passed, plasticity is activated and the stress remains equal to Σ'_c . Accordingly, (Σ_f, K^d) is the set of parameters to be identified.

Identification is performed numerically using Monte Carlo simulations for Bayesian inference based on a random walk Metropolis-Hastings sampling algorithm Robert and Casella (2004). Note that \mathcal{M}_2 is not a trilinear model because of the continuum damage model (see e.g. Ibrahimbegovic (2009) for details on the numerical implementation of continuum damage models). The following parameters have been identified as the expected a posteriori (expectation of the posterior parameter distribution): for \mathcal{M}_1 , $\mu = 30.5$ MPa and $s = 28.8$ MPa, and for model \mathcal{M}_2 , $\Sigma_f = 16.32$ MPa and $K^d = 14.4$ GPa. How the numerical models match the experimental data is shown in figure 9. From these pictures, one can draw the observations gathered in table 1. We recall that a simplified version of model \mathcal{M}_2 is used here and that enhanced performance can be expected from the full version of \mathcal{M}_2 .

4.3 Discrepancy forces

Two models for the analyzed column (see figure 6) are built with same steel behavior law and both concrete laws \mathcal{M}_1 and \mathcal{M}_2 introduced in section 2 with the coefficients identified in section 4.2.3.

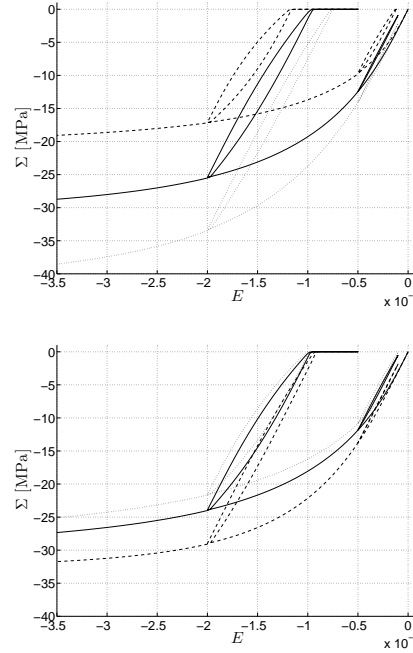


Figure 8: Macro-scale concrete response for different targeted values for the mean μ and standard deviation s of the random field: [top] $\mu = 24.5$ (- -), 35.0 (—), 45.5 (· · ·) MPa and $s = 51.9$ MPa; [bottom] $\mu = 35$ MPa and $s = 35.0$ (- -), 51.9 (—) and 78.3 (· · ·) MPa.

The recorded time histories during shaking table test consist in the horizontal relative displacement (y^e) and relative acceleration (\ddot{y}^e) at the top of the analyzed column, along with the shaking table acceleration (\ddot{u}_g). Resisting forces \mathbf{f}^{hys} in the column are computed solving the following quasi-static nonlinear problem:

$$\begin{pmatrix} 0 \\ \mathbf{0} \\ \mathbf{0} \end{pmatrix} := \begin{pmatrix} f^{sta,e} + F \\ \mathbf{f}^{sta,f} \\ \mathbf{f}^{ext,b} \end{pmatrix} - \begin{pmatrix} f^{hys,e}(y^e, \mathbf{y}^f, \mathbf{0}) \\ \mathbf{f}^{hys,f}(y^e, \mathbf{y}^f, \mathbf{0}) \\ \mathbf{f}^{hys,b}(y^e, \mathbf{y}^f, \mathbf{0}) \end{pmatrix} \quad (9)$$

where the displacement y^e is applied to the structure, F is the reaction to this imposed displacement and \mathbf{f}^{sta} is the static part of the external loading. Static loading is applied before and kept constant during seismic motion.

Due to a lack of recorded data, we assume that dynamic effects for the vertical and rotational DOFs at the top of the column can be

Damping model-free analysis of a stochastic multi-scale frame element for earthquake engineering
P. Jehel, H. Vincent, and T. Rodet

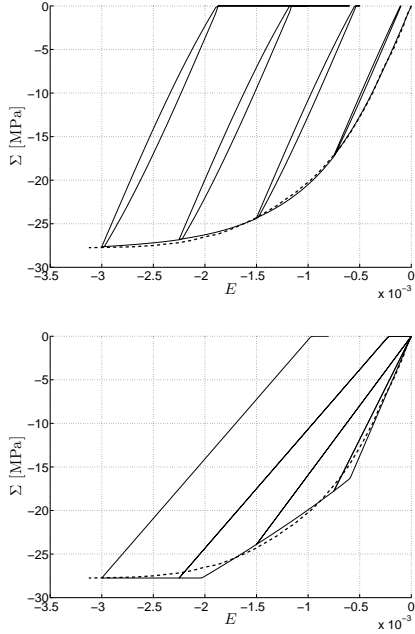


Figure 9: Dashed line represents the experimental backbone curve; there is no experimental data available for the unloading-reloading cycles. For same loading path: [top] Fitted model \mathcal{M}_1 (mean of 2,000 meso-structures); [bottom] Fitted model \mathcal{M}_2 .

neglected, that is $\ddot{\mathbf{y}}^f = \mathbf{0}$. Finally, using the experimentally recorded accelerations \ddot{y}^e and \ddot{u}_g , the discrepancy forces \mathbf{f}^{dis} are computed: introducing equations (9) in equations (8) along with the assumption $\ddot{\mathbf{y}}^f = \mathbf{0}$, it comes:

$$\begin{pmatrix} f^{dis,e} \\ \mathbf{f}^{dis,f} \\ \mathbf{f}^{dis,b} \end{pmatrix} := \begin{pmatrix} f^{sta,e} - M \ddot{u}_g \\ \mathbf{f}^{sta,f} \\ \mathbf{f}^{ext,b} \end{pmatrix} - \begin{pmatrix} M \ddot{y}^e \\ \mathbf{0} \\ \mathbf{0} \end{pmatrix} - \begin{pmatrix} f^{sta,e} + F \\ \mathbf{f}^{sta,f} \\ \mathbf{f}^{ext,b} \end{pmatrix} \quad (10)$$

Accordingly, $\mathbf{f}^{dis,f} = \mathbf{f}^{dis,b} = \mathbf{0}$ and

$$f^{dis,e} = -M (\ddot{y}^e + \ddot{u}_g) - F \quad (11)$$

$f^{dis,e}$ provides a damping model-free quantity that can be used as a measure of the capacity of the column model to represent the behavior that has been experimentally observed during shaking table test. If the structural model

Feature	\mathcal{M}_1	\mathcal{M}_2
Backbone curve	accurate	fair
Local hysteresis	yes	no
Loss of stiffness	no	yes
Residual def.	yes	yes

Table 1: Comparative analysis of the capability of models \mathcal{M}_1 and \mathcal{M}_2 to reproduce salient features of the compressive cyclic response of a concrete specimen. “Local hysteresis” is used for “hysteresis in unloading-reloading cycles”.

were capable of perfectly representing the experimental response of the analyzed column, discrepancy forces would be null. The lack of experimental information about the vertical and rotational DOFs introduces some uncertainty in the computation of $f^{dis,e}$, which unlike the uncertainty brought by the damping model in a direct time history seismic analysis could be tackled by using complementary experimental data.

Discrepancy force $f^{dis,e}$ is computed for the column modeled either with concrete model \mathcal{M}_1 or \mathcal{M}_2 . Figure 10 shows $F(t)$ and $f^{dis,e}(t)$ for both models. One can observe that, in the structure with model \mathcal{M}_1 , both the reaction and the discrepancy forces are lower than in the structure with model \mathcal{M}_2 . Theoretically, the lower the discrepancy forces, the more accurate the structural model, which leads to conclude that model \mathcal{M}_1 better grasps the actual physical mechanisms in concrete than model \mathcal{M}_2 . Nevertheless, this conclusion is counterbalanced by the other fact that these forces have been computed according to some hypotheses that are likely to introduce errors in the results, such as zero-rotation at the top end of the column. With additional data collected during the shaking table test, these errors could however be removed. Note finally that, very roughly, the computation of the reactions $F(t)$ with model \mathcal{M}_2 is a matter of less than a minute on standard laptop with 2.53 GHz processor whereas it takes several but less than ten minutes with model \mathcal{M}_1 .

5 Conclusions

In this paper, the capability of a fiber element with an inelastic stochastic multi-scale nonlin-

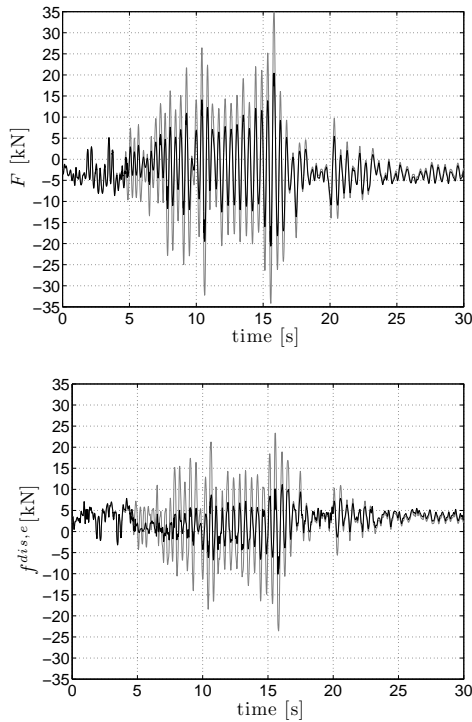


Figure 10: Black is for the column with concrete model \mathcal{M}_1 , gray with model \mathcal{M}_2 . Horizontal reactions with imposed relative displacement y^e [top] and discrepancy forces pertaining to the horizontal DOF [bottom] at the top of the column.

ear concrete material model to numerically represent the seismic response of a reinforced concrete column observed during shaking table test is investigated. For the sake of comparison, same analysis is carried out using a more classical inelastic concrete model with internal variables. The results of such an investigation can be biased by the uncertainty brought by the damping forces added in inelastic time history seismic analyses. The concept of discrepancy forces for computational mechanics problems allows for removing this uncertainty. Nevertheless, due to a lack of recorded experimental data, some assumptions have to be made before calculating the discrepancy forces, which also introduces errors in the analysis. However, these latter errors, unlike those coming from uncertain damping forces, could be removed with complementary experimental measures.

The stochastic multi-scale nonlinear concrete material model used in this work simulates a uniaxial behavior at macro-scale that results from the homogenization of a spatially variable response at meso-scale. This spatial variability is conveyed by the fluctuations of a 2D homogeneous non-Gaussian random field. Some parameters of the digitized random field are set so that response at macro-scale is almost independent of the realization of the meso-structure. The mean and standard deviation of the marginal log-normal distribution selected for generating the random fields are identified with Bayesian inference along with MCMC simulations to fit experimental concrete uniaxial compressive response.

The numerical simulations presented in this paper lie in-between the two following bounds, both of which are related to the need for further experimental investigation:

- (i) At small scales, interaction with material scientists is necessary to collect experimental evidence that would support the choices made to account for the heterogeneous nature of concrete (correlation function, inelastic response at meso-scale, marginal distribution, random parameter,...).
- (ii) At large scales, interaction between experts in computational mechanics and experts in the design of experimental seismic tests is necessary for experimental protocol and finite element model to be jointly designed at an early stage in the analysis process, so that there is sufficient experimental data recorded to compute the discrepancy forces at a maximum of the DOFs of the finite element model.

Acknowledgements

First author is supported by a Marie Curie International Outgoing Fellowship within the 7th European Community Framework Programme (proposal No. 275928). Second author is supported by the French Ministry of Higher Education and Research as a pupil of ENS Cachan. Both supports are gratefully acknowledged. First two authors also thank Prof. Deodatis at Columbia University for hosting them during the preparation of this work.

Damping model-free analysis of a stochastic multi-scale frame element for earthquake engineering
 P. Jehel, H. Vincent, and T. Rodet

References

- Benkemoun, N., Hautefeuille, M., Colliat, J.-B., and Ibrahimbegovic, A. (2010). Failure of heterogeneous materials: 3D meso-scale FE models with embedded discontinuities. *International Journal for Numerical Methods in Engineering*, 82:1671–1688.
- Charmpis, D. C., Schuëller, G. I., and Pellissetti, M. F. (2007). The need for linking micromechanics of materials with stochastic finite elements: A challenge for materials science. *Computational Materials Science*, 41:27–37.
- Charney, F. A. (2008). Unintended consequences of modeling damping in structures. *Journal of Structural Engineering*, 134(4):581–592.
- Computers & Structures Inc. (2007). *Perform3D User’s manual*. Berkeley, CA, USA.
- Davenne, L., Ragueneau, F., Mazars, J., and Ibrahimbegovic, A. (2003). Efficient approaches to finite element analysis in earthquake engineering. *Computers and Structures*, 81:1223–1239.
- FEMA P695 (2009). Quantification of building seismic performance factors. Technical Report FEMA P695.
- Filiatrault, A., Lachapelle, E., and Lamontagne, P. (1998). Seismic performance of ductile and nominally ductile reinforced concrete moment resisting frames. I. Experimental study. *Canadian Journal of Civil Engineering*, 25:331–341.
- Hall, J. F. (2006). Problems encountered from the use (or misuse) of Rayleigh damping. *Earthquake Engineering and Structural Dynamics*, 35:525–545.
- Ibrahimbegovic, A. (2009). *Nonlinear Solid Mechanics: Theoretical Formulations and Finite Element Solution Methods*. Springer.
- Jehel, P. (2013). A look into uncertainty in structural seismic performance arising from additional Rayleigh damping in inelastic time history analysis. In Deodatis, G., Ellingwood, B. R., and Frangopol, D. M., editors, *Proceedings of the 11th International Conference on Structural Safety and Reliability (ICOSSAR)*, New York. CRC Press.
- Jehel, P. (2014). A critical look into rayleigh damping forces for seismic performance assessment of inelastic structures. *Engineering Structures*, In press.
- Jehel, P. and Cottureau, R. (2015). On damping created by heterogeneous yielding in the numerical analysis of nonlinear reinforced concrete frame elements. *Submitted*.
- Jehel, P., Davenne, L., Ibrahimbegovic, A., and Léger, P. (2010). Towards robust viscoelastic-plastic-damage material model with different hardenings / softenings capable of representing salient phenomena in seismic loading applications. *Computers and Concrete*, 7(4):365–386.
- Jehel, P., Léger, P., and Ibrahimbegovic, A. (2014). Initial versus tangent stiffness-based Rayleigh damping in inelastic time history seismic analyses. *Earthquake Engineering and Structural Dynamics*, 43:467–484.
- Jeremić, B., Sett, K., and Kavvas, M. L. (2007). Probabilistic elasto-plasticity: formulation in 1D. *Acta Geotechnica*, 2:197–210.
- Lee, T.-H. and Mosalam, K. M. (2005). Seismic demand sensitivity of reinforced concrete shear-wall building using FOSM method. *Earthquake Engng Struct. Dyn.*, 34:1719–1736.
- Maugin, G. (1999). *The Thermodynamics of Nonlinear Irreversible Behaviors – An Introduction*. World Scientific. River Edge, Singapore.
- Ramtani, S. (1990). *Contribution to the modeling of the multi-axial behavior of damaged concrete with description of the unilateral characteristics*. PhD Thesis (in French), Paris 6 University.
- Richard, B. and Ragueneau, F. (2013). Continuum damage mechanics based model for quasi brittle materials subjected to cyclic loadings: Formulation, numerical implementation and applications. *Engineering Fracture Mechanics*, 98:383–406.
- Robert, C. and Casella, G. (2004). *Monte Carlo Statistical Methods*. Springer, New York, 2 edition.
- Shinozuka, M. and Deodatis, G. (1996). Simulation of multi-dimensional Gaussian stochastic fields by spectral representation. *Applied Mechanics Reviews*, 49(1):29–53.
- Simo, J. C. and Hughes, T. J. R. (1998). *Computational Inelasticity*. Springer, Berlin.
- Stroeven, P., Hu, J., and Chen, H. (2008). Stochastic heterogeneity as fundamental basis for the design and evaluation of experiments. *Cement & Concrete Composites*, 30:506–514.
- Taylor, R. L., Filippou, F. C., Saritas, A., and Auricchio, F. (2003). A mixed finite element method for beam and frame problems. *Computational Mechanics*, 31:192–203.
- Wong, P. S. and Vecchio, F. J. (2002). *VecTor2 & Formworks User’s Manuals*. University of Toronto, Department of Civil Engineering, Toronto, ON, Canada.